Redox-dependent Structural Origins of the Temperature Threshold and Sensitivity in the TRPV3 Bio-thermometer

Guangyu Wang (gary.wang10@gmail.com)
University of California Davis https://orcid.org/0000-0002-5581-6926

Research Article

Keywords: hairpin thermodynamics, lipid, non-covalent interaction, redox-dependence, thermo-sensitivity, threshold, TRP channel, use-dependent sensitization

Posted Date: August 3rd, 2022

DOI: https://doi.org/10.21203/rs.3.rs-1556082/v10

Redox-dependent Structural Origins of the Temperature Threshold and Sensitivity in the TRPV3 Bio-thermometer

Guangyu Wang*

Department of Physiology and Membrane Biology, University of California School of Medicine, Davis, CA, USA

Department of Drug Research and Development, Institute of Biophysical Medico-chemistry, Reno, NV, USA

* Author to whom correspondence should be addressed; E-mail: gary.wang10@gmail.com

Abstract

The DNA hairpin with a limited size or strength is sensitive to temperature. However, it is unclear if thermosensitive TRP channels also use the temperature-dependent little hairpin sizes or strengths to govern their temperature thresholds and sensitivity. Here, graph theory was used as a novel tool to test this hypothesis by analyzing the redox- and state-dependent cryo-electron microscopy structures of mouse TRPV3 with or without the Y564A mutation at different temperatures. The results showed that the biggest little hairpin with the minimal topological loop size and strength determines the temperature threshold while a change in the total minimal little hairpin sizes upon a change in the total little hairpin-dependent non-covalent interactions along the channel gating pathway governs the temperature sensitivity. This size- and strength-dependent hairpin thermodynamics may tune the thermal activity and sensitivity of biological macromolecules. (136 words)

Significance

The temperature thresholds and sensitivity of the thermosensitive transient receptor potential channels are often mediated by non-covalent interactions including H-bonds, salt bridges and aromatic π interactions at different ambient temperatures. Although their relative complexity has made them challenging to study, graph theory and hairpin thermodynamic modelling have now

reached the stage at which we can explain their physical origins and gain reliable insight into the effects of the little hairpin size and strength on the thermo-stability of those non-covalent interactions along the channel gating pathway. This computational study offers opportunities for us to understand how temperature manipulates these complex non-covalent interactions and their direct incorporation into the design of bio-thermometers protects our bodies from noxious heat or cold damages. (119 words)

Category: computational biochemistry; biophysics; graph theory; network analysis; redox regulation; structural bioinformatics

Keywords: hairpin thermodynamics; lipid; non-covalent interaction; temperature sensitivity; threshold; TRP channel

1. INTRODUCTION

The transient receptor potential (TRP) channels can be gated by both physical and chemical stimuli to conduct cations. Among 28 mammalian members in the TRP superfamily, eleven ones are thermosensitive through a variety of TRP channel families including TRPV (vanilloid), TRPM (melastatin), TRPC (canonical), and TRPA (ankyrin). Their temperature thresholds (T_{th}) for activation range from noxious cold, cold, warm to noxious heat. Specifically, TRPV1 (>42°C), TRPV2 (>52°C), TRPV3 (>32–39°C), TRPV4 (>25–35°C), TRPM2, TRPM3, TRPM4, and TRPM5 are involved in warm to hot sensation. In contrast, TRPA1 (<17°C) or TRPM8 (<20–28°C) and TRPC5 (<25-37°C) are sensitive to cold and cool temperatures. These thermosensitive TRP channels also have a high temperature sensitivity Q_{10} compared to non-temperature-sensitive ones [1-16]. However, the origins of their temperature threshold and sensitivity are unknown.

A critical clue comes from a DNA hairpin thermal biosensor. Its hairpin size within 20 bases in a loop can produce a temperature threshold in a range of those thermosensitive TRP channels. The larger hairpin size and the less H-bonds in the stem generally have a lower threshold. Its initial melting curve also has a characteristic slope as the temperature sensitivity (Q_{10}=1.8-2.7) [17]. Therefore, it is exciting to ask if the temperature-dependent biggest little hairpin with a minimal loop size and strength along the gating pathway of the thermosensitive TRP channel initiates an activation threshold while a change in the total minimal little hairpin sizes between closed and open states of a single channel upon a change in the total little hairpin-dependent non-covalent interactions controls Q_{10}. The recent state- and redox-dependent cryo-electron microscopy (cryo-EM) structures of mTRPV3 with or without the Y564A mutation at different temperatures may provide an opportunity for graph theory to be used as a novel tool to examine the hypothesis [18-20]. In addition, mTRPV3 undergoes sensitization while TRPV1, 2 and 4 channels desensitize upon successive heat stimuli [7, 18-24]. Thus, the role of the redox state of mTRPV3 in use-dependent sensitization was also investigated. Once such a hairpin thermodynamic model was applied to this thermo-gated cation channel, the calculated melting temperatures (T_m) and structural thermo-sensitivity (Ω_{10}) values were commensurable to the experimental thresholds (T_{th}) and functional thermo-sensitivity (Q_{10}) values, respectively. In this regard, TRPV3 may use a change of the temperature-dependent biggest little hairpin to detect different ambient temperatures with a high sensitivity.

2. RESULTS

2.1. The Definition of the Least Gating Pathway of mTRPV3

mTRPV3 is mainly expressed in skin keratinocytes and oral and nasal epithelia, mediating thermal reception and pain sensation [5-6]. Like other TRPV channels, TRPV3 is a homotetramer. Each monomer has S1-S6 as a transmembrane domain (TMD) and a large intracellular amino- (N-) terminal as an ankyrin repeat domain (ARD). S1-S4 form a voltage-sensor-like domain (VSLD) while S5-S6 and the pore helix and two pore loops are folded as a pore domain. Both the VSLD and the pore domain are swapped via a S4-S5 linker. The TRP helices, which are almost parallel to the membrane, interact with both the skirt ARD and the TMD. Several lipid sites were also found in their interfaces. The pre-S1 domain, together with the carboxyl- (C-) terminal loop domain, couples the TMD with the ARD. The residues ^{638}GLGD^{641} in the P-loop-extended region line the selectivity filter to permeate partially hydrated Na^+ , K^+ or Ca^{2+} ions but not to function as an upper gate. In contrast, the narrowest pore constriction around M677 on S6 may act as a lower gate. Since the interaction of the pre-S1 domain with the TRP domain constitutes a sealed large loop so that a heat-evoked conformational change can be extended along the loop, the least gating pathway of mTRPV3 should include at least the pre-S1 domain and the TRP domain. [18, 21]

2.2. The First Biggest Little Hairpin in the VSLD/pre-S1 Interface Set a Temperature Threshold 40°C for Oxidized mTRPV3

C612 and C619 in the outer pore of mTRPV3 can form a disulfide bond upon oxidization [18]. In the closed state at 42°C, the diversity of non-covalent interactions between amino acid side chains in oxidized mTRPV3 could produce multiple little hairpins along the gating pathway from D396 in the pre-S1 domain to K505 in the TRP domain.

First, H-bonds emerged between different hydrophilic residues. In the pre-S1/TRP interface, the H-bonding pairs T397-K432/E704 sealed the largest hairpin loop from T397 to E704. In the VSLD, the H-bonding pairs included T456-W559 and K500-E501. In the S4-S5 linker/TRP interface two H-bonding pairs R567-T699 and E689-R693 were found. In the pore domain, H-bonds were formed among pairs including D586-T680, Y594-T636-Y661, E610/K614-N647, S621-Q646, and E682-K686 (Fig. 1A).

Second, several aromatic residues were involved in π interactions with nearby residues. For example, W433-R696/K438 in the TRP/pre-S1 interface, F441-W433/Y565 in the pre-S1/VSLD interface, F445-F449/Y565, F447/Y451-W493, Y448-Y451/F526/Y565, F449/N452-W559, Y460-Y461, H471-Y540/Y547, F489-W493, W521-F522, F522/Y564-F526, F524-V528,

F527-V531, Y540-Y547, F542-Y544, and Y564-Y565 in the VSLD, Q570/R696-W692 and Y575-I579 in the S4-S5 linker/TRP interface, F590-Y594/L673, F597-F601/L664, F601/T665-Y661, Y622/Q646-F654, F625-V629, T649-Y650, and F656-T660 in the pore domain (Fig. 1A). In addition, the vanilloid site phosphatidylcholine (PC) also related W521 on S3 to Q695 in the TRP domain via a CH-π interaction and an H-bond, respectively (Fig. 1A-B).

Third, salt bridges were also present between several charged pairs. They covered D396/E704-K432 in the TRP/pre-S1 interface, R416-D519 in the VSLD/pre S1 interface, E610-K614 in the outer pore, and R698-E702 in the TRP domain (Fig. 1A).

Taken together, despite several smallest little hairpins with no residue in the loops, the first biggest little hairpin with a minimal 17-residue loop appeared in the VSLD/pre-S1 interface to control the D519-R416 salt bridge (Fig. 1C-D). It started with D519 and went through W521, F522, Y564, Y565, F441, W433 and ended with R416 (Fig. 1E). Based on two equivalent H-bonds sealing the loop, the predicted melting temperature was about 40°C, which was close to the threshold 36-42°C for the activation of oxidized mTRPV3 (Table 1). [18] The total numbers of all non-covalent interactions and little hairpin sizes with minimal loops along the gating pathway from D396 to K705 were 60 and 83, respectively (Fig. 1A).

2.3. Oxidized mTRPV3 Opened at 42°C with a Low Sensitivity upon the 1st Biggest Little Hairpin Melting

In the heat-activated open state, when the disruption of the R416-D519 salt bridge melted the first biggest little hairpin at 42°C as predicted (Table 1), several changes were observed with the release of the PC lipid from nearby W521 and Q695 in oxidized mTRPV3.

First, in the VSLD/pre-S1/TRP interfaces, the D519-R416 salt bridge was substituted by the T411-R416 and D519-R567 H-bonds. As a result, the T397/E704-K432 H-bonds and the D396-K432 salt bridge were broken with the formation of H417/E418-R690 and E423-T427 H-bonds. In addition, the K432-E704 salt bridge became an H-bond (Fig.2A).

Second, when R567 formed a stimulatory H-bond with D519 in the VSLD, a little hairpin with a minimal 2-residue loop appeared from D519 to W521, F522, Y564, Y565, R567 and back to D519. As a result, the V528-F524 and F522-F526 π interactions were disconnected (Fig. 2A).

Third, when the conformational wave extended to the S4-S5/TRP interfaces, the R567-T699 H-bond and the Y575-I579 π interaction were disrupted while the E689-R693 H-bond was changed to a salt bridge (Fig. 2A).

Table 1 The hairpin thermodynamic model-based new parameters of the mTRPV3 bio-thermometer along the gating pathway from D396 to K705

Construct	**mTRPV3**			**mTRPV3-Y564A**	
PDB ID	6LGP	7MIO	7MIN	6PVP	6PVO
Lipid PC at the vanilloid site	bound	free	bound	free	free
Redox state	reduced	oxidized	oxidized	reduced	reduced
Lipid environment	MSP2N2	cNW11	cNW11	detergent	
Sampling temperature	**4°C**	**42°C**	**42°C**	**37°C**	**37°C**
Gating state	**Closed ↔ Open ↔ Closed**			**Open ↔ Closed**	
# of the biggest little hairpin	3	2	1	5	4
Biggest little loop size (L_{max}), a.a/carbon	12	9	17	11	13
Equivalent H-bonds in L_{max}	2.0	2.0	2.0	2.5	1.0
Total non-covalent interactions	60	52	60	41	39
Total little hairpin sizes, a.a/carbon	95	66	83	78	80
Calculated melting temperature (T_m)	**50°C**	56°C	**40°C**	57°C	**38°C**
Measured temperature threshold (T_{th})	**50-52°C**		**36-42°C**		**37°C**
Calculated $\Omega_{10,\,min}$ at E_{min}=0.5 kJ/mol	9.76		5.44		0.52
Calculated $\Omega_{10,\,mean}$ at E_{mean}=1.0 kJ/mol	**21.7**		**11.7**		**1.00**
Calculated $\Omega_{10,\,max}$ at E_{max}=3.0 kJ/mol	76.6		44.2		2.84
Measured $Q_{10,}$	**22.1-26.9**		**?**		**1.21**
Ref. for measured T_{th} or Q_{10}	[19, 26]		[18]		[19]

Fourth, when this conformational wave continued to the pore domain, those F597-F601 π interaction and N647-E610/K614 and E682-K686 H-bonds and the E610-K614 salt bridge were disconnected. In the meanwhile, the E631-K634 H-bond and the F633-I637 π interaction were present, and the H-bond moved from S621-Q646 to S620-Q646 pairs with the shift of the π interaction from T649-Y650 to Y650-L653 (Fig. 2A).

Taking together, after the first biggest little hairpin with a minimal 17-residue loop in the VSLD/pre-S1 interface melted above the predicted 40°C, the biggest little hairpin moved to the S5-S6 interface (Fig. 2B-C). When two equivalent H-bonds sealed a minimal 9-residue loop from D586 to F590 and L673 and T680 and back to D586 (Figs. 2C, E), the calculated melting temperature was about 56°C (Table 1). In the meanwhile, a little hairpin with a minimal 3-residue

loop in the pre-S1/VSLD/S4-S5 linker/TRP/pre-S1 interfaces may be required to stimulate the lower state of the channel. It linked multiple active residues together such as W433, F441, Y565, Y564, F522, W521, D519, R567, Q570, W692, R696 (Figs. 2D, 2E). As a result, the total numbers of all non-covalent interactions and minimal little hairpin sizes along the gating pathway from D396 to K705 decreased from 60 and 83 to 52 and 66, respectively (Fig. 2A). Such a decrease produced a low structural thermo-sensitivity Ω_{10} in a range from 5.44 to 44.2 and with a mean value 11.7 (Table 1).

2.4. Reduced mTRPV3 had a High Structural Thermo-sensitivity and the Third Biggest Little Hairpin in the VSLD

In the closed state without the C612-C619 disulfide bond, reduced mTRPV3 at 4°C was different than oxidized one. In the pore domain, when the E610-K614 salt bridge and the E610-N647 and S621-Q646 H-bonds were disrupted, the F633-I637 π interaction and the Y594-Y661 H-bond emerged (Fig. 3A).

When this conformational change extended to the S4-S5 linker/TRP/S6 interfaces, the R698-E702 salt bridge and the R567-T699 and E682-K686 H-bonds were broken but the T566-S576 and Q570-E689 H-bonds were created (Fig.3A). As a result, in the VSLD/pre S1 interface, when the T397-K432 H-bond was disrupted, D519 formed an additional H-bond with T411. In the VSLD, when the T456-W559 H-bond was disconnected, the H471-Y540/Y547 π interactions changed to the Y448/Y551-Q519 H-bonds, the π interaction moved from F542-Y544 to Y540-Y544, and the H-bond shifted from K500-E501 to Q514-S518. When the PC bridge moved from W521-PC-Q695 to W521-PC-F524/R567, H523 formed a lone pair-π interaction with E501 in the presence of the Y564-R567 π interaction. Of special note, D519 in the S2-S3 linker generated a salt bridge with R698 in the TRP domain. More importantly, in addition to a salt bridge between R567 and the PC lipid, the CH-π interactions of the PC lipid with W521 and F524 brought about the third biggest little hairpin with two equivalent H-bonds sealing a minimal 12-carbon loop (Fig. 3B-D). The predicted melting temperature was about 50°C (Table 1), in agreement with the initial experimental threshold 50-52°C for TRPV3 opening. [26] On the other hand, reduced mTRPV3's total numbers of all non-covalent interactions and minimal hairpin sizes along the gating pathway from D396 to K705 were 60 and 95, respectively (Fig. 3A). When the same open state was employed (Fig.2A), the calculated structural thermo-sensitivity Ω_{10} was in a range from 9.76 to

76.6 and with a mean value 21.7, which was comparable to the experimental functional thermo-sensitivity Q_{10} (22.1-26.9) (Table 1). [19, 26]

2.5. Release of the PC Lipid from the Vanilloid Site by the Y564A Mutation Decreased the Melting Threshold of the Biggest Little Hairpin to Activate Reduced mTRPV3

When reduced mTRPV3 had a mutation Y564A on S4, the disruption of the Y564-F522/F526/Y565/R567 π interactions not only released the PC lipid from the vanilloid site but also induced several changes along the gating pathway from D396 to K705 (Fig. 4A)[19]. In the VSLD, when the F522-F526 and Y540-Y544/Y547 π interactions were disconnected, the π interactions shifted from W521-F524 to W521-V525 and from W493-Y451 to F489-F450 but the E501-H523 π interaction became an H-bond. Even if the Q514-S518 H-bond was also broken, F526 still had a π–π interaction with Y565, and the T456-W559 H-bond was also reinstated with the replacement of the Y448-Y451 and Y460-Y461 π interactions with the F441-F445 π interaction. In the VSLD/S4-S5linker/TRP interfaces, the T566-S576 and Q570-E689 H-bonds and the Q570-W692-R696 and Y575-I579 π interactions were disrupted with the formation of a salt bridge between E687 and R690. In the TRP/pre-S1/VSLD/TRP interfaces, when the D519-R698 salt bridge was broken, the T397-E704 and T411-D519 H-bonds and the K432-E704 salt bridge and the F441-W433 π interaction were substituted by the Y409-R698 and T421-R690 H-bonds. Of special note, K500 formed a salt bridge with E702 (Fig.4A).

When these conformational changes expanded to the pore domain, the broken non-covalent interactions included the Y594/T636-Y661 and K614-N647 H-bonds, and the F597-F601 and Y622-F654 and F633-I637 π interactions. In the presence of the Y622-S626 H-bond, the π interactions shifted from Q646-F654 to N647-F654 and from T649-Y650 to Y650-I652 pairs (Fig.4A). Of note, L632 produced a CH-π interaction with Y666 (Fig.4A).

As a result, the fourth biggest little hairpin with one equivalent H-bond sealing a minimal 13-residue loop appeared in the pre-S1/TRP interface (Fig.4B). It controlled the D396-K432 salt bridge via the Y409-R698 H-bond (Fig. 4C-D). In this case, the removal of the PC lipid from the vanilloid site decreased the temperature threshold from 50°C to 38°C as calculated (Table 1). This melting temperature was near the experimental threshold 37°C [19]. In the meanwhile, the total numbers of all non-covalent interactions and minimal little hairpin sizes along the gating pathway from D396 to K705 also reduced from 60 and 95 to 39 and 80, respectively (Fig. 4A).

2.6. Release of the PC Lipid from the Vanilloid Site by the Y564A Mutation Decreased the Structural Thermo-sensitivity of Reduced mTRPV3

When the mTRPV3-Y564A mutant opened with the fourth biggest little hairpin melting in the TRP/pre-S1 interface at 37°C, the disruption of the D396-K432 salt bridge triggered several changes. In the VSLD/pre-S1/TRP/VSLD interfaces, the R416-D519 H-bond changed to the D519-R698 salt bridge, and the Y409-R698 and T421-R690 H-bonds were substituted by the H417-E689 π interaction. When T411 H-bonded with S515, the E702-K500 salt bridge became an H-bond. In the S4-S5 linker/TRP interface, the R567-Q695 H-bond and the Q570-W692-R696 π interactions appeared with the broken E689-R693 H-bond (Fig. 5A).

When these conformational changes extended to the pore domain, the D586-K589 H-bond and the E631-K634 salt bridge were born with the restoration of F597-F601 π interaction and the Y594-Y661-T636 H-bonds. However, the Y622-S626 and N647-F654 π interactions were disrupted (Fig. 5A).

When the conformational wave expanded to the VSLD, the F445-Y565 and F449-W559 and F450-F489 π interactions and the T456-W559 H-bond were disrupted but both the R464-D468 salt bridge and the H477-W481 π interaction were present. On the other hand, when the W521-F522 and F524-V528 π interactions were disconnected, the F522-F526 and Y540-Y547 and F542-Y544 π interactions appeared again (Fig. 5A).

By all accounts, two little hairpins may favor opening. One with a minimum 4-residue loop from D519 to W521, V525, F626, Y565, R567, Q695, R698 and back to D519 in the VSLD/TRP interface (Figs. 5A-B. 5E); The other was the fifth biggest little hairpin in the TRP/VSLD/pre-S1 interfaces to control the H417-E689 π interaction. It had a minimal 11-residue loop from T411 to H417, E689, W692, R696, R698, D519, S515, and back to T411 (Figs. 5A, 5C-E). Once 2.5 equivalent H-bonds sealed the loop, the melting temperature was about 57°C (Table 1). In any way, the total numbers of all non-covalent interactions and minimal little hairpin sizes along the gating pathway from D396 to K705 had only minor changes from 39 and 80 to 41 and 78, respectively (Fig. 5A). In this case, the calculated structural thermo-sensitivity Ω_{10} was in a range from 0.52 to 2.84 and with a mean value 1.00, which was comparable to the experimental functional thermo-sensitivity Q_{10} (~1.21). [19] In other words, the removal of the PC lipid from the vanilloid site by the Y564A mutation dramatically weakened the structural and functional thermo-sensitivities.

3. DISCUSSION

Although protein and DNA use sequences of amino acids and nucleotides to form primary polypeptide and polynucleotide chains, respectively, an alteration in the loop sequence has no significant effect on the melting temperature of the DNA hairpin. [17] Therefore, when an intramolecular non-covalent interaction creates a topological hairpin, the hairpin should be thermodynamically and chemically equivalent between DNA and protein.

At a given salt concentration (150 mM NaCl), a DNA hairpin with a 20-base long poly-A loop has a temperature threshold 34°C. When the loop size decreases from 20 to 10 bases or the H-bonded base pairs in the stem increase from 2 to 4, the threshold can be increased more than 20 degrees. [17] If the biggest little hairpin undergoes a single-step melting reaction similarly to DNA hairpins to initiate a temperature threshold for mTRPV3 activation, the calculated melting temperature (T_m) should be comparable to the experimental threshold (T_{th}) for channel activation. In agreement with this proposal, for reduced mTRPV3, the calculated T_m of the third biggest little hairpin with 2.0 equivalent H-bonds sealing a minimal 12-carbon loop was 50°C. This value was similar to the initial T_{th} 50-52°C for reduced mTRPV3 activation. [26] For oxidized mTRPV3, the calculated T_m of the first biggest little hairpin with 2.0 equivalent H-bonds sealing a minimal 17-residue loop was about 40°C, which was close to the experimental T_{th} 36-42°C. [18] When the Y564A mutation removes the PC lipid from the vanilloid site, the fourth biggest little hairpin with 1.0 equivalent H-bond sealing a minimal 13-residue loop resulted in a calculated T_m 38°C, which was near the experimental threshold 37°C (Table 1). [19] On the other hand, the calculated T_m values of the second and fifth biggest little hairpins in the open states were about 56°C and 57°C, respectively (Figs. 2, 5), allowing the measurable range of thermo-gated mTRPV3 to be at least from 40°C to 56°C (Table 1). Therefore, the biggest little hairpins along the gating pathway may be responsible for not only the temperature thresholds but also the measureable range of the mTRPV3 bio-thermometer in redox- and PC lipid-dependent manners.

Since a smaller hairpin has a higher melting temperature and thus a larger heat capacity [17], if Q_{10} of mTRPV3 results from the decrease in the total minimal loop sizes in little hairpins along the gating pathway upon a concurrent change in the total little hairpin-dependent non-covalent interactions, the defined and calculated structural thermo-sensitivity Ω_{10} should be comparable to the functional thermo-sensitivity Q_{10}. In accordance with this notion, reduced mTRPV3 has an experimental Q_{10} value 22.1-26.9 while the calculated mean Ω_{10} was about 21.7. [19, 26] When

this channel was oxidized, the Ω_{10} value was decreased to 11.7. For reduced mTRPV3-Y564A, the Q_{10} and Ω_{10} values were 1.21 and 1.00, respectively. [19] In this regard, when the intensity of a non-covalent interaction was in the range from 0.5 to 3 kJ/mol, the Q_{10} ranges from the minimum to the maximum may be theoretically calculated as 9.76-76.6 for reduced mTRPV3, 5.44-44.2 for oxidized mTRPV3, and 0.52-2.84 for reduced mTRPV3-Y5674A (Table 1).

It has been reported that mTRPV3 exhibits the high temperature threshold (T_{th}, 50-52°C) and the sensitivity ($Q_{10,}$ 22.1) in response to the first heat stimulus. [26] In this case, C612 may have formed a disulfide bond with C619 in the open state upon the initial activation, decreasing the temperature threshold from 50°C to 40°C and the structural thermo-sensitivity from 21.7 to 11.7 for the second stimulus (Figs 1-3, Table 1). [18] On the other hand, like mTRPV3-Y564A mutant, the release of the PC lipid from the vanilloid site in the open state also lowered down the threshold and sensitivity to 38°C and 1.00 for the second thermo-gated activation, respectively (Figs. 4-5, Table 1). [19] Since the subsequent experimental Q_{10} value is about 2.32, [26] even if oxidization between C612 and C619 had decreased the temperature sensitivity to 11.7, the release of the PC lipid from the vanilloid site may still be required for the very low sensitivity of mTRPV3 in response to the second warm stimulus (Table 1). [26] In any way, the lower threshold below 40°C may increase the open probability in response to the same temperature jump so that mTRPV3 activation exhibits use-dependent sensitization upon successive heat stimuli [18, 26].

In addition to the biggest little hairpins for the thresholds, smaller little hairpins may be needed for heat-evoked mTRPV3 opening. Some were state- and redox-independent no matter whether the stimulus is physical or chemical (Figs. 1-3). Therefore, they may form a basic stable backbone anchor system for mTRPV3 activation or a fuse group to prevent heat denaturation or channel deactivation [18-20].

The first had two residues in the loop from Y594 to T636, Y661, T665, L664, F597 and back to Y594. The mutation N643S, I644S, N647Y, L657I, or Y661C in the outer pore is factually less sensitive to heat [27], possibly by destablizing that smaller little hairpin and thus decreasing the heat efficacy (Fig. 2). In addition, the T636S mutation also decreases the temperature threshold [28], possibly by forming the new biggest little hairpin with a size larger than 12-carbon in the minimal loop or weakening non-covalent interactions to seal the biggest little hairpin loop along the gating pathway (Fig.3).

The second had a minimal 9-residue loop from D586 to F590, L673 and T680 and then back to D586 (Fig. 2A). In line with this importance, the T680A mutation suppresses the heat-evoked opening of reduced mTRPV3 with the N-terminal 1–117 residues truncated [25].

The third had a minimal 4-residue loop from T411 to R416 and D519 and then back to T411 (Fig. 3A). When the insertion of valine or serine at position 412 disrupts the T411-D519 H-bond, another biggest little hairpin with a minimal 17-residue loop from R416 to D519, W521, F522, Y564, Y565, F441, W433 may be formed in the VSLD/pre-S1/TRP interfaces and thus dramatically decrease the threshold and sensitivity like oxidized mTRPV3 (Figs.1-3, Table 1). [19, 26]

The fourth had no residue in the loop from Y448 to F526, Y564, Y565 and back to Y448 (Figs. 1-3). It has been reported that the Y564A mutation decreases the threshold of reduced mTRPV3 from 50°C to 37°C and the temperature sensitivity Q_{10} from 22.1 or 26.9 to 1.21 (Table 1). [19, 26].

Finally, further experiments may be required to test if non-covalent interactions in other smaller little hairpins are essential for heat-evoked TRPV3 opening. For example, the D519-R416 salt bridge, the H417/E418-R690 and D519-R567 and S620-Q646 H-bonds, the F441/F445/Y448-Y565 and F449-W559 and H471-Y540/Y547 and Y622/Q646-F654 π–π interactions, and the W692-R696-W433-K438 cation-π interactions (Fig. 2A).

4. METHODS

4.1 Data Mining Resources

In this computational biochemical study, the cryo-EM structural data of oxidized mTRPV3 with a high resolution in different gating and redox states at 42°C were first analyzed with graph theory, a novel tool, to reveal the roles of the little hairpins with minimal loop sizes and strengths in regulating the temperature threshold and the thermosensitivity of TRPV3. They include closed and reduced mTRPV3 in MSP2N2 (PDB ID, 6LGP, model resolution= 3.31 Å), [25] closed and oxidized mTRPV3 in cNW11 (PDB ID, 7MIN, model resolution= 3.09 Å), and open and oxidized mTRPV3 in cNW11 (PDB ID, 7MIO, model resolution= 3.48 Å) [18]. In addition, the cryo-EM structural data of detergent-solubilized and reduced mTRPV3-Y564A in the sensitized but closed state (PDB ID, 6PVO, model resolution= 5.18 Å) and in the open state at 37°C (PDB ID, 6PVP, model resolution= 4.4 Å) were also analyzed as controls to uncover the role of the PC lipid in increasing the temperature threshold and sensitivity of TRPV3 [19].

4.2 Standards for Non-covalent Interactions

Structure visualization software, UCSF Chimera, was used to assess the presence of non-covalent interactions in TRPV3. Since the gating of thermosensitive TRP channels is governed by stereo- or regioselective inter- or intradomain interactions, only stereo- or regioselective diagonal and lateral non-covalent interactions were included in this study to test their potential roles in forming minimal little hairpin topological loops to control the temperature threshold and sensitivity. They included salt-bridges, CH/cation/lone pair/π–π interactions and H-bonds along the gating pathway in mTRPV3 with or without the Y564A mutation. In contrast, the hydrophobic interactions were not considered because they lack both stereo- and regio-selectivity [29].

The standard definition of noncovalent interactions was employed. A hydrogen bond was considered present when the angle donor-hydrogen-acceptor was within the cut-off of 60°, and when the hydrogen-acceptor distance is within 2.5 Å and the maximal distance is 3.9 Å between a donor and an acceptor. A salt bridge was considered to be formed if the distance between any of the oxygen atoms of acidic residues and the nitrogen atoms of basic residues were within the cut-off distance of 3.2-4 Å in at least one frame. When the geometry was acceptable, a salt bridge was also counted as a hydrogen bonding pair. The face-to-face π-π stacking of two aromatic rings was considered effective once the separation between the π-π planes was ~3.35-4.4 Å, which is close to at least twice the estimated van der Waals radius of carbon (1.7Å). The edge-to-face π-π interaction of two aromatic rings was considered attractive when the cut-off distance between two aromatic centers was within 4-6.5 Å. Significant cation-π interactions occurred within a distance of 6.0 Å between a cation and an aromatic center. The short effective CH/π distances was 2.65-3.01 Å between aromatic groups, and 2.75-2.89 Å between CH_3 and an aromatic ring. The lone pair-π interaction distance between a lone electron pair and an aromatic ring was within 3-3.7 Å.

4.3 Preparation of Little Hairpin Topological Loop Maps by Using Graph Theory

After non-covalent interactions were scanned along the gating pathway of mTRPV3 from D396 in the pre-S1 domain to K705 in the TRP domain, graph theory was used as a novel tool to define the minimal loop size in little hairpins to control every non-covalent interaction and geometrically to realize the little hairpin topological loop maps along the gating pathway in the closed, sensitized or open states at 4°C, 37°C and 42°C. The primary amino acid sequence line from D396 to K705 was marked in black. An amino acid side chain or an atom of a bound lipid involving a non-covalent interaction along the gating pathway of rTRPV1 was represented as a

vertex (v) or a node and marked with an arrow in different colors. The same kind of non-covalent interactions was marked in the same color. Any link between two vertices was represented an edge in a biochemical network. A hairpin topologicval loop was formed between two vertices *i* and *j* (v_i and v_j), if and only if there was a path from v_i to v_j and a return path from v_j to v_i. The loop path length (L) was definded as the total number of residues or atoms in the bound lipid that do not participate in any non-covalent interctions in a little hairpin loop. For a given biochemical reaction network, the minimal loop path length (L_{min}) between v_i and v_j was the sum of the shortest return path distance from node *j* to i because the direct shortest path distance from node *i* to *j* was zero when a non-covalent interaction existed between them. The simplest way to find the minimal loop was to identify the shortest return path between two vertices *i* and *j* (v_i and v_j) by using the Floyd-Warshall algorithm. [30] For example, in the biochemical reaction network of Fig.1A, a direct path length from E610 and N647 was zero because there was an H-bond between them. However, there was another shortest return path from N647 to K614 and back to E610 via another H-bond and a salt bridge but no residues in this loop. Therefore, the minimal little hairpin loop path length was zero. After each non-covalent interaction was tracked by a minimal loop length and marked in black, the total number of all noncovalent interactions and minimal hairpin loop lengths along the gating pathway were shown in black and blue circles, respectively.

4.4 Calculation of the Temperature Threshold of mTRPV3

The temperature threshold was calculated from the melting temperature T_m of the biggest little hairpin along the gating pathway using the following equation: [17]

$$T_m\ (°C) = 34 + (n-2)\times 10 + (20-L_{max})\times 2$$

where, n is the total number of the non-covalent interactions equivalent to H-bonds in the biggest little hairpin, and L_{max} is the loop length of the biggest little hairpin.

4.5 Calculation of the Temperature Sensitivity of mTRPV3

If a thermosensitive ion channel changes from a closed state to an open state within a temperature range ΔT, $\Omega_{\Delta T}$ was defined to evaluate the structural thermo-sensitivity of a single ion channel as calculated using the following equation:

$$\Omega_{\Delta T} = [(L_c - L_o)E/2]^{(Nc/No)}$$

where, L_c and L_o are the total numbers of all the minimal lengths of little hairpins along the gating pathway in the closed and open states, respectively; N_c and N_o are the total numbers of all the non-

covalent interactions along the gating pathway in the closed and open states, respectively; E is the energy intensity of a non-covalent interaction in a range of 0.5-3 kJ/mol. Usually, E=1 kJ/mol.

When $\Delta T=10°C$, Ω_{10} could be comparable to the functional thermo-sensitivity Q_{10} of a single ion channel. Q_{10} was calculated using the following equation:

$$Q_{10} = (R2/R1)^{10/(T2-T1)}$$

where, R1 and R2 are rates of a reaction at two different temperatures T1 and T2 in Celsius degrees or kelvin, respectively.

Conventions and Abbreviations: ARD, ankyrin repeat domain; cryo-EM, cryo-electron microscopy; T_m, melting temperature; PC, phosphatidylcholine; T_{th}, temperature threshold; TMD, transmembrane domain; TRP, transient receptor potential; TRPV3, TRP vanilloid-3; mTRPV3, mouse TRPV3; VSLD, voltage-sensor-like domain.

Acknowledgements

The author's own studies cited in this article were supported by NIDDK Grant (DK45880 to D.C.D.) and Cystic Fibrosis Foundation grant (DAWSON0210) and NIDDK grant (2R56DK056796-10) and American Heart Association (AHA) Grant (10SDG4120011 to GW).

Conflict of Interest: The author declares no conflict of interest.

Data Availability Statement: All data generated or analysed during this study are included in this published article.

References

1. Caterina, M.J., Schumacher M.A., Tominaga M., Rosen T.A, Levine J.D. and Julius D. The capsaicin receptor: a heat-activated ion channel in the pain pathway. *Nature*. (1997) **389(6653),** 816-824.
2. Caterina, M.J., Rosen T. A., Tominaga M., Brake A. J, Julius D. A capsaicin-receptor homologue with a high threshold for noxious heat. *Nature.* (1999) **398,**436.
3. McKemy D. D., Neuhausser W. M. & Julius D. Identification of a cold receptor reveals a general role for TRP channels in thermosensation. *Nature.* (2002) **416(6876),** 52–58.
4. Peier, A.M., Moqrich A., Hergarden A.C., Reeve A.J., Andersson D.A., Story G.M., Earley T.J., Dragoni I., McIntyre P., Bevan S. and Patapoutian A. A TRP channel that senses cold stimuli and menthol. *Cell*. (2002) **108(5),** 705–715.
5. Peier A. M., Reeve A. J., Andersson D.A., Moqrich A., Earley T.J., Hergarden A.C., Story G.M., Colley S., Hogenesch J. B., McIntyre P., Bevan S., Patapoutian A. A heat-sensitive TRP channel expressed in keratinocytes. *Science*. (2002) **296,** 2046.
6. Smith G. D., Gunthorpe M. J., Kelsell R. E., Hayes P. D., Reilly P., Facer P., Wright J. E., Jerman J. C., Walhin J-P., Ooi L., Egerton J., Charles K. J., Smart D., Randall A. D., Anand P., Davis J. B. TRPV3 is a temperature-sensitive vanilloid receptor-like protein. *Nature.* (2002) **418,** 186.
7. Xu H., Ramsey I. S., Kotecha S. A., Moran M. M., Chong J. A., Lawson D., Ge P., Lilly J., Silos-Santiago I., Xie Y., DiStefano P. S., Curtis R., Clapham D. E. TRPV3 is a calcium-permeable temperature-sensitive cation channel. *Nature.* (2002) **418,** 181.
8. Guler A.D., Lee H., Iida T., Shimizu I., Tominaga M.and Caterina M. J. Heat-evoked activation of the ion channel, TRPV4. *J Neurosci.* (2002) **22,** 6408–14.
9. Chung M. K., Lee H., Caterina M. J. Warm temperatures activate TRPV4 in mouse 308 keratinocytes. *J. Biol. Chem*. (2003) **278,** 32037.
10. Story, G.M., Peier A.M., Reeve A.J., Eid S.R., Mosbacher J., Hricik T.R., Earley T.J., Hergarden A.C., Andersson D.A., Hwang S.W., McIntyre P., Jegla T., Bevan S., Patapoutian A. ANKTM1, a TRP-like channel expressed in nociceptive neurons, is activated by cold temperatures. *Cell*. (2003) **112,** 819–829.

11. Jordt, S.E., Bautista D.M., Chuang H.H., McKemy D.D., Zygmunt P.M., Högestätt E.D., Meng I.D. and Julius D. Mustard oils and cannabinoids excite sensory nerve fibres through the TRP channel ANKTM1.*Nature.* (2004) **427,** 260–265.
12. Talavera K, Yasumatsu K., Voets T., Droogmans G., Shigemura N., Ninomiya Y., Margolskee R. F., Nilius B. Heat activation of TRPM5 underlies thermal sensitivity of sweet taste. *Nature.* (2005) **438,** 1022.
13. Vriens J, Owsianik G., Hofmann T., Philipp S., Stab J., Chen X., Benoit M., Xue F., Janssens A., Kerselaers S., Oberwinkler J., Vennekens R., Gudermann T., Nilius B., Voets T. TRPM3 is a nociceptor channel involved in the detection of noxious heat. *Neuron.* (2011) **70,** 482.
14. Zimmermann,K., Lennerz J.K., Hein A., Link A.S., Kaczmarek J.S., Delling M., Uysal S., Pfeifer J.D., Riccio A. and Clapham D.E. Transient receptor potential cation channel, subfamily C, member 5 (TRPC5) is a cold-transducer in the peripheral nervous system. *Proc. Natl. Acad. Sci.USA*. (2011) **108,** 18114–18119.
15. Song K., Wang H., Kamm G. B., Pohle J., Reis F. C., Heppenstall P., Wende H., Siemens J. The TRPM2 channel is a hypothalamic heat sensor that limits fever and can drive hypothermia. *Science.* (2016) **353,**1393.
16. Tan C. H., McNaughton P. A. The TRPM2 ion channel is required for sensitivity to warmth. *Nature.* (2016) **536,** 460.
17. Jonstrup A.T., Fredsøe J., Andersen A.H. DNA Hairpins as Temperature Switches, Thermometers and Ionic Detectors. *Sensors.* (2013) **13,** 5937-5944.
18. Nadezhdin, K. D., Neuberger, A., Trofimov, Y. A., Krylov, N. A., Sinica, V., Kupko, N., Vlachova, V., Zakharian, E., Efremov, R. G., and Sobo-levsky, A. I. Structural mechanism of heat-induced opening of a temperature-sensitive TRP channel. *Nat. Struct. Mol. Biol.* (2021) **28,** 564–572.
19. Singh, A.K., McGoldrick L.L., Demirkhanyan L., Leslie M., Zakharian E., and Sobolevsky A.I. Structural basis of temperature sensation by the TRP channel TRPV3. *Nat. Struct. Mol. Biol.* (2019) **26,** 994–998.
20. Singh, A.K., McGoldrick L.L. and Sobolevsky A.I. Structure and gating mechanism of the transient receptor potential channel TRPV3. *Nat. Struct. Mol. Biol.* (2018) **25,** 805–813.

21. Zubcevic, L., Herzik Jr. M. A., Wu M., Borschel W.F., Hirschi M., Song A.S., Lander G.C., and Lee S. Y. Conformational ensemble of the human TRPV3 ion channel. *Nat. Commun.* (2018**) 9,** 4773.
22. Liao M, Cao E., Julius D. & Cheng Y. Structure of the TRPV1 ion channel determined by electron cryo-microscopy. *Nature.* (2013) **504,**107.
23. Liu B.Y., Yao J., Zhu M.X. & Qin F. Hysteresis of gating underlines sensitization of TRPV3 channels. *J. Gen. Physiol.* (2011) **138,** 509–520.
24. Liu B. & Qin F. Use dependence of heat sensitivity of vanilloid receptor TRPV2. *Biophys J.* (2016) **110(7),** 1523–1537.
25. Shimada, H., Kusakizako, T., Nguyen, THD, Nishizawa, T., Hino T., Tominaga M., Nureki, O. The structure of lipid nanodisc-reconstituted TRPV3 reveals the gating mechanism. *Nat Struct Mol Biol.* (2020) **27,** 645-652.
26. Liu, B. & Qin F. Single-residue molecular switch for high-temperature dependence of vanilloid receptor TRPV3. *Proc. Natl.Acad. Sci. USA.* (2017) **114,** 1589–1594.
27. Grandl JH, Hu H, Bandell M, Bursulaya B, Schmidt M, Petrus M and Patapoutian A. Pore region of TRPV3 ion channel is specifically required for heat activation. *Nat. Neurosci*. (2008) **11,** 1007–1013.
28. Myers B. R., Bohlen C. J., Julius D. A yeast genetic screen reveals a critical role for the pore helix domain in TRP channel gating. *Neuron.* (2008) **58,** 362-273.
29. Baumgartner A. Insertion and Hairpin Formation of Membrane Proteins: A Monte Carlo Study. *Biophys. J.* (1996**) 71,** 1248-1255.
30. Floyd RW.) Algorithm-97 - Shortest Path. *Commun Acm* (1962), **5,** 345–345.

Figure legends

Figure 1. **The little hairpin topological structural network along the gating pathway of PC-bound oxidized mTRPV3 in the closed state at 42°C. A,** The little hairpin topological loop map. The cryo-EM structure of closed and oxidized mTRPV3 with PC bound in cNW11 at 42°C (PDB ID, 7MIN) was used for the model.[18] The pore domain, the S4-S5 linker, the TRP domain, the VSLD and the pre-S1 domain are indicated in black. Salt bridges, π interactions, and H-bonds between pairing amino acid side chains along the gating pathway from D396 to K705 are marked in purple, green, and orange, respectively. The minimal loop sizes in the little hairpins required to control the relevant non-covalent interactions are labeled in black. The total numbers of all minimal little hairpin loop sizes and non-covalent interactions along the gating pathway are shown in the blue and black circles, respectively. **B,** The PC lipid at the vanilloid site. **C,** The location of the 1st biggest little hairpin is marked in a red circle. **D,** The structure of the 1st biggest little hairpin with a minimal 17-residue loop in the VSLD/pre S1 interface to control the R416-D519 salt bridge. **E,** The sequence of the 1st biggest little hairpin with a minimal 17-residue loop. The R416-D519 salt bridge is marked in a blue box.

Figure 2. **The little hairpin topological structural network along the gating pathway of PC-free oxidized mTRPV3 in the open state at 42°C. A,** The little hairpin topological loop map. The cryo-EM structure of open mTRPV3 without PC bound in cNW11 at 42°C (PDB ID, 7MIO) was used for the model.[18] The pore domain, the S4-S5 linker, the TRP domain, the VSLD and the pre-S1 domain are indicated in black. Salt bridges, π interactions, and H-bonds between pairing amino acid side chains along the gating pathway from D396 to K705 are marked in purple, green, and orange, respectively. The minimal loop sizes in the little hairpins required to control the relevant non-covalent interactions are labeled in black. The total numbers of all minimal little hairpin loop sizes and non-covalent interactions along the gating pathway are shown in the blue and black circles, respectively. **B,** The location of the 2nd biggest little hairpin is marked in a red circle. **C,** The structure of the 2nd biggest little hairpin with a minimal 9-residue loop in the S5-S6 interface to control the stimulatory D586-T680 H-bond. **D,** The structure of the putative little hairpin with a minimal 3-residue loop for the lower gate. **E,** The sequences of two little gating

hairpins with minimal 9- and 3-residue loops to control the D586-T680 H-bond and two crtitical non-covalent interactions in the blue boxes, respectively.

Figure 3. **The little hairpin topological structural network along the gating pathway of PC-bound reduced mTRPV3 in the closed state at 4°C. A,** The little hairpin topological loop map. The cryo-EM structure of reduced and closed mTRPV3 with PC bound in MSP2N at 4°C (PDB ID, 6LGP) was used for the model.[25] The pore domain, the S4-S5 linker, the TRP domain, the VSLD and the pre-S1 domain are indicated in black. Salt bridges, π interactions, and H-bonds between pairing amino acid side chains along the gating pathway from D396 to K705 are marked in purple, green, and orange, respectively. The minimal loop sizes in the little hairpins required to control the relevant non-covalent interactions are labeled in black. The total numbers of all minimal little hairpin loop sizes and non-covalent interactions along the gating pathway are shown in the blue and black circles, respectively. The T411-D519 H-bond, which is marked in a dashed line, may be disrupted by the insertion of valine or serine at position 412. **[26] B,** The location of the 3rd biggest little hairpin is marked in a red circle. **C,** The structure of the 3rd biggest little hairpin with a minimal 12-carbon loop in the VSLD to control the W521-PC-F524 bridge. **D,** The sequences of the 3rd biggest little hairpin with a minimal 12-carbon loop to control the W521-PC-F524 bridge in the blue rectangle.

Figure 4. **The little hairpin topological structural network along the gating pathway of PC-free reduced mTRPV3-Y564A in the sensitized but closed state at 37°C. A,** The little hairpin topological loop map. The cryo-EM structure of detergent-solubilzed and sensitized and reduced mTRPV3 without PC bound at 37°C (PDB ID, 6PVO) was used for the model.[19] The pore domain, the S4-S5 linker, the TRP domain, the VSLD and the pre-S1 domain are indicated in black. Salt bridges, π interactions, and H-bonds between pairing amino acid side chains along the gating pathway from D396 to K705 are marked in purple, green, and orange, respectively. The minimal loop sizes in the little hairpins required to control the relevant non-covalent interactions are labeled in black. The total numbers of all minimal little hairpin loop sizes and non-covalent interactions along the gating pathway are shown in the blue and black circles, respectively. **B,** The location of the 4th biggest little hairpin is marked in a red circle. **C,** The structure of the 4th biggest little hairpin with a minimal 13-residue loop in the TRP/pre S1 interface to control the D396-K432 salt

bridge. **D,** The sequence of the 4th biggest little hairpin with a minimal 13-residue loop to control the D396-K432 salt bridge in the blue rectangle.

Figure 5. **The little hairpin topological structural network along the gating pathway of PC-free reduced mTRPV3-Y564A in the open state at 37°C. A,** The little hairpin topological loop map. The cryo-EM structure of detergent-solubilzed and open mTRPV3-Y564A without PC bound in cNW11 at 37°C (PDB ID, 6PVP) was used for the model.[19] The pore domain, the S4-S5 linker, the TRP domain, the VSLD and the pre-S1 domain are indicated in black. Salt bridges, π interactions, and H-bonds between pairing amino acid side chains along the gating pathway from D396 to K705 are marked in purple, green, and orange, respectively. The minimal loop sizes in the little hairpins required to control the relevant non-covalent interactions are labeled in black. The total numbers of all minimal little hairpin loop sizes and non-covalent interactions along the gating pathway are shown in the blue and black circles, respectively. **B,** The structure of a little hairpin with a minimal 4-residue loop for the D519-R698 salt bridge. **C,** The location of the 5th biggest little hairpin is marked in a red circle. **D,** The structure of the 5th biggest little hairpin with a minimal 11-residue loop in the VSLD/TRP/pre S1 interfaces to control the H417-E689 H-bond. **E,** The sequences of two little gating hairpins with minimal 4- and 11-residue loops to control the D519-R698 salt bridge and the H417-E689 H-bond in the blue boxes, respectively.

Figures

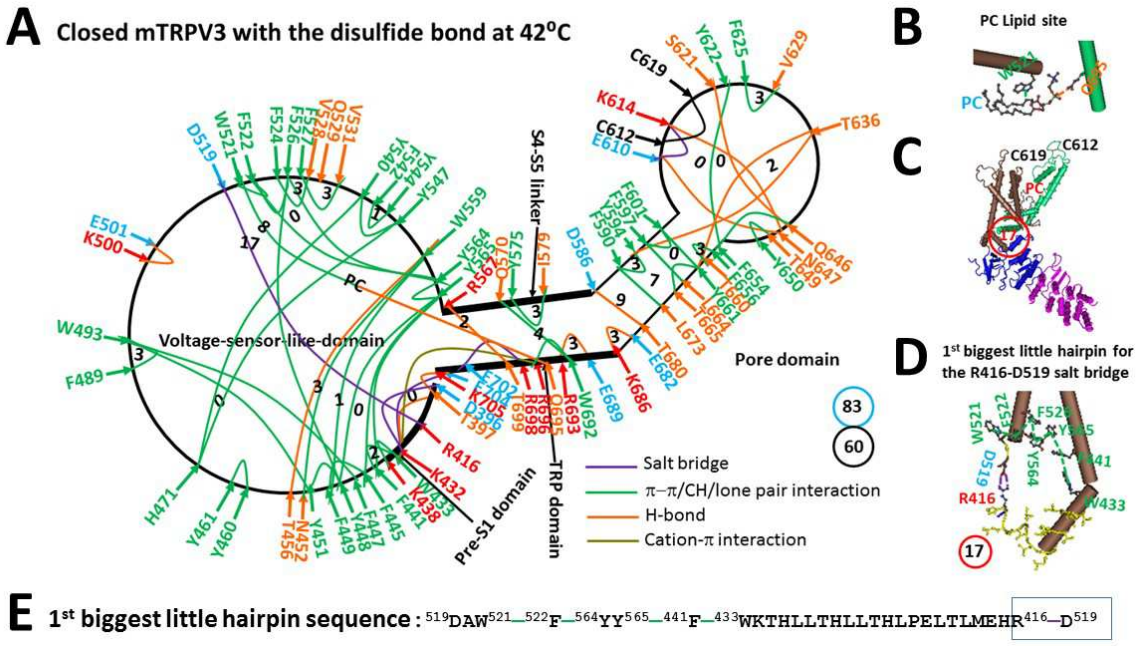

Figure 1

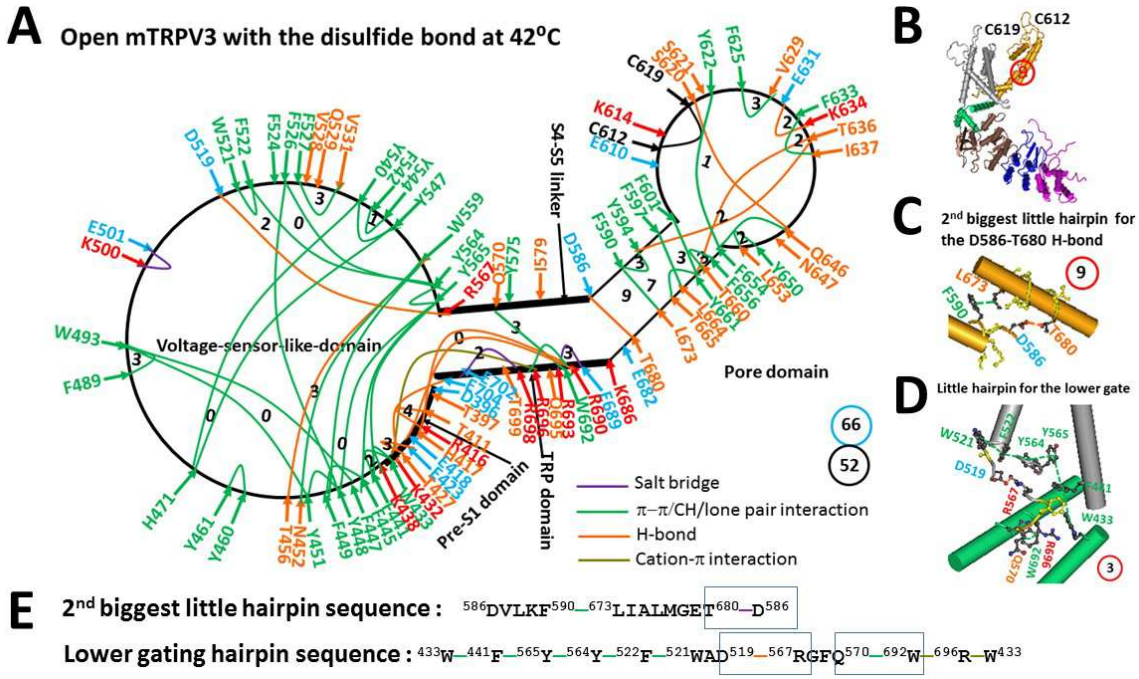

Figure 2

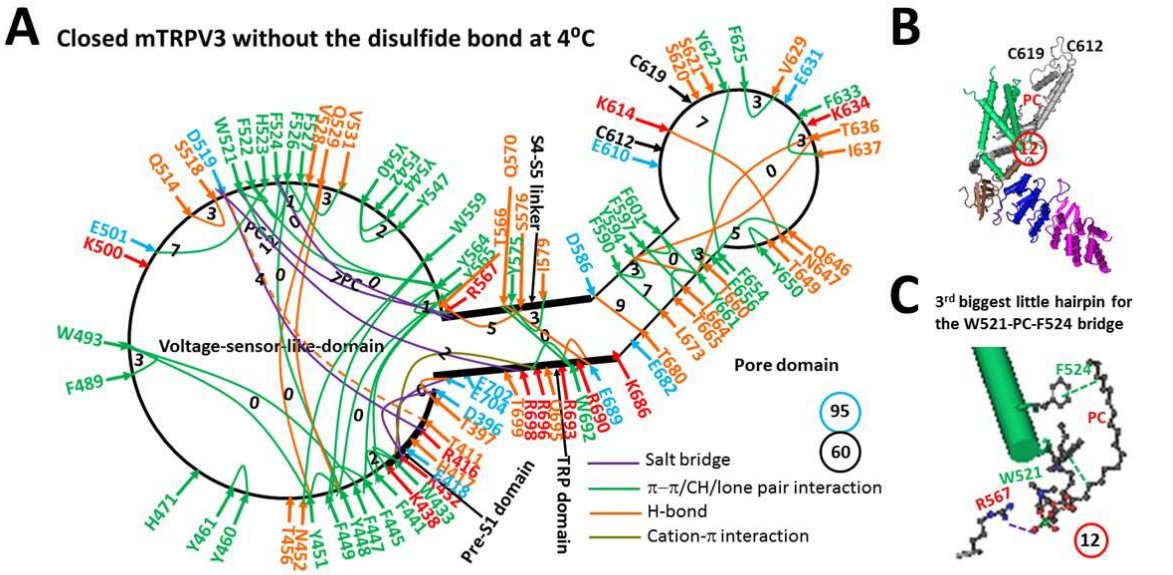

D 3rd biggest little hairpin sequence : ^{521}W–PC–F^{524}–W^{521}

Figure 3

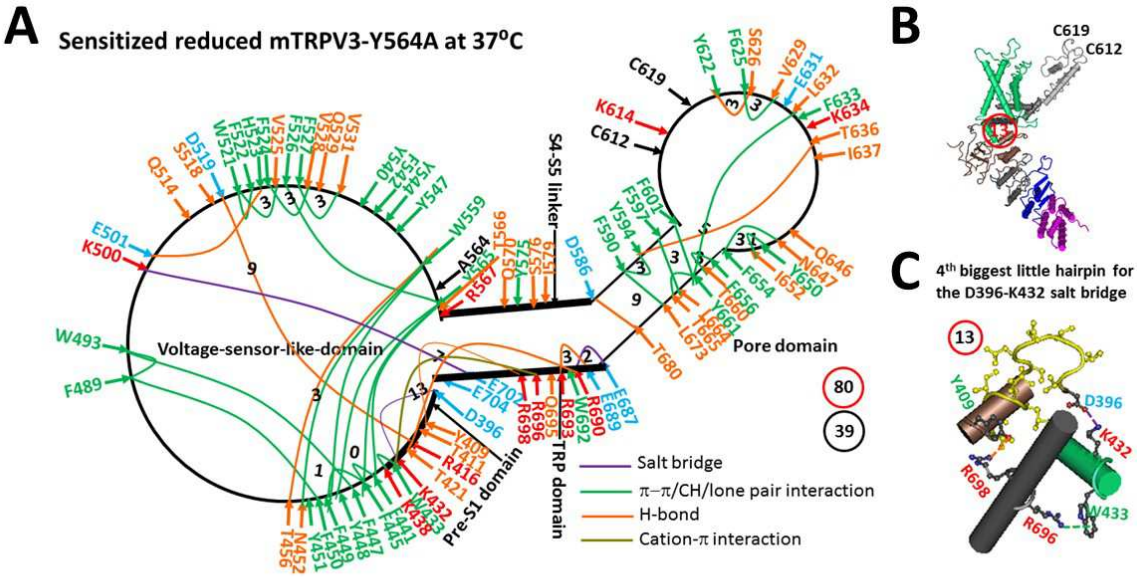

D 4th biggest little hairpin sequence : ^{396}DTTTDNSVLEIIVY^{409}–^{698}RAR^{696}–^{433}WK^{432}–^{396}D

Figure 4

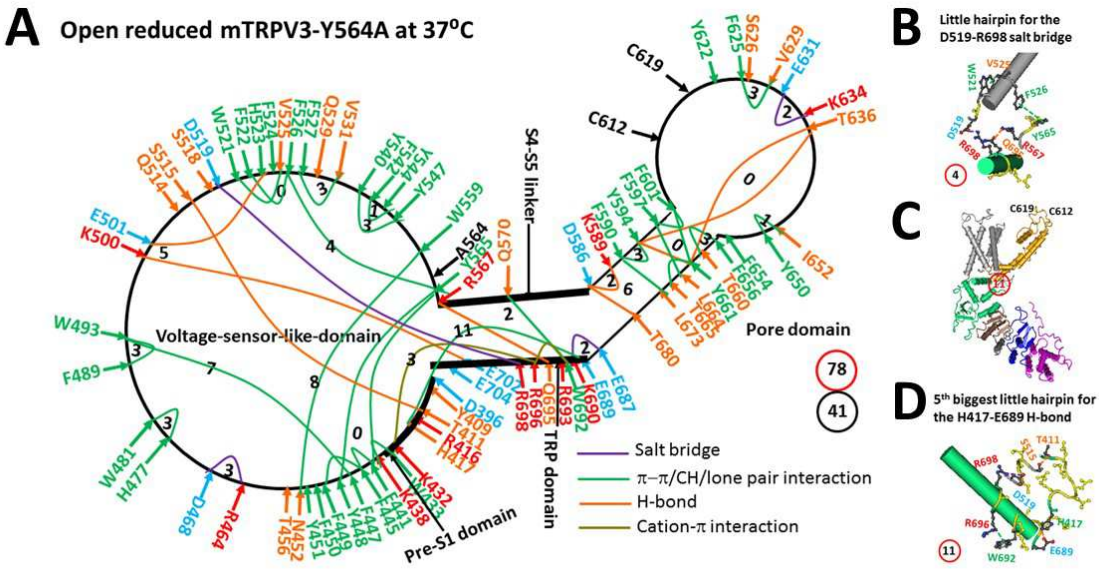

E **Little hairpin sequence :** ^{519}DAW^{521}_^{525}VF^{526}_^{565}YTR^{567}_^{695}QRAR^{698}–D^{519}

5th biggest little hairpin sequence : ^{411}TNIDNRH^{417}_^{689}EKIW^{692}_^{696}RAR^{698}_^{519}DSLIS^{515}_^{411}T

Figure 5